

Biocompatible Peptide Coated Ultra-Small Superparamagnetic Iron Oxide Nanoparticles for *in vivo* Contrast-Enhanced Magnetic Resonance Imaging

*Heng Li Chee,^{a,†} Ching Ruey R. Gan,^{a,†} Michael Ng,^b Lionel Low,^c David G. Fernig,^d Kishore K. Bhakoo,^b
and David Paramelle^{e,*}*

^aInstitute of Materials Research and Engineering, A*STAR (Agency for Science, Technology and Research), 2 Fusionopolis Way, Innovis #08-03, 138634, Singapore

^bSingapore Bioimaging Consortium, A*STAR (Agency for Science, Technology and Research), 11 Biopolis Way, 138667, Singapore

^cSingapore Immunology Network, A*STAR (Agency for Science, Technology and Research), 8a Biomedical Grove, 138648, Singapore

^dDepartment of Biochemistry, Institute of Integrative Biology, University of Liverpool, Liverpool, L69 7ZB, United Kingdom

ABSTRACT The biocompatibility and performance of reagents for *in vivo* contrast-enhanced magnetic resonance imaging are essential for their translation to the clinic. The quality of the surface coating of nanoparticle-based MRI contrast agents, such as ultra-small superparamagnetic iron oxide nanoparticles (USPIONs), is critical to ensure high colloidal stability in biological environments, improved magnetic

performance and dispersion in circulatory fluids and tissues. Herein, we report the design of a library of 21 peptides and ligands and identify highly stable self-assembled monolayers on the USPIOs surface. A total of 86 different peptide coated USPIOs are prepared and selected using several stringent criteria, *e.g.*, stability against electrolyte-induced aggregation in physiological conditions, prevention of non-specific binding to cells, absence of cellular toxicity and contrast-enhanced *in vivo* MRI. The bis-phosphorylated peptide 2PG-S*VVVT-PEG4-ol provides highest biocompatibility and performance for USPIOs, with no detectable toxicity or adhesion to live cells. The 2PG-S*VVVT-PEG4-ol coated USPIOs show enhanced magnetic resonance properties, r_1 ($2.4 \text{ mM}^{-1} \cdot \text{s}^{-1}$) and r_2 ($217.8 \text{ mM}^{-1} \cdot \text{s}^{-1}$) relaxivities, and greater r_2/r_1 relaxivity ratios (>90), when compared to commercially available MRI contrast agents. Furthermore, we demonstrate the utility of 2PG-S*VVVT-PEG4-ol coated USPIOs as a T2 contrast agent for *in vivo* MRI applications. High contrast enhancement of the liver is achieved as well as detection of liver tumors, with significant improvement of the contrast-to-noise ratio of tumor-to-liver contrast. It is envisaged that the reported peptide coated USPIOs have the potential to allow for the specific targeting of tumors, and hence early detection of cancer by MRI.

KEYWORDS: peptide, coating, iron oxide nanoparticles, biocompatibility, magnetic resonance imaging.

The development of safe and high-performing nanoparticle-based contrast agents for medical imaging¹ and their translation to the clinic offers high potential to greatly improve both diagnosis and treatment, also known as theranostic,² of various diseases such as cancer and neurological pathologies. Superparamagnetic iron oxide nanoparticles (SPIONs) are the most successful nanomaterial-based contrast agents translated today for human utilization for T2-weighted magnetic resonance imaging (MRI), and are generally considered for both diagnosis and therapeutic uses.³⁻¹⁰ Importantly, ultra-small superparamagnetic iron oxide nanoparticles (USPIOs) have been proposed as an alternative to the well-established gadolinium-based contrast agents (GBCA) for MRI, particularly for patients with chronic kidney diseases at risk of nephrogenic systemic fibrosis.¹¹ In spite of the growing variety of SPION formulations approved

by the Food and Drug Administration (FDA) for use in humans as iron deficiency therapeutics or as MRI contrast agents, *e.g.*, Feridex®, Umirem®, Resovist®, the constant reevaluation of the potential risk of side-effects and efficacy led in most cases to their subsequent withdrawal from the market.¹² It is thus critical to further improve the biocompatibility and performance of SPIONs and create innovative solutions enabling their translation for clinical utilization.

The coating of USPIOs is a key component to ensure biocompatibility and maintenance of high performance during *in vivo* imaging. The coating protects the USPIOs core from a challenging biological environment, hence preventing any undesired decomposition or aggregation. The coating may also control their interactions with the body's tissues and fluids, and allow the USPIOs to target specific organs and areas in the body, *e.g.*, tumors. During MRI acquisition, the proximity of protons to the water present in tissues and the USPIOs surface facilitates the signal. Hence the quality and thickness of the USPIOs coating influences the magnetic performance of the contrast agent.¹³ Current FDA-approved SPIONs are formulated as either individual or cluster of iron oxide nanoparticles encapsulated in highly hydrophilic synthetic or biological polymers, *e.g.*, polyethylene glycol, polysaccharides, dextran.^{3,14,15} Despite the numerous advantages of polymer coatings, *e.g.*, biocompatibility, increased hydrophilicity and further bio-functionalization,¹⁶ such formulations may increase their hydrodynamic size and potentially affect their magnetic resonance performance.¹³

We have previously demonstrated the utilization of well-designed short peptides and ligands to form highly stable and thin self-assembled monolayers (SAM) for the coating of noble metal nanoparticle probes dedicated to bioimaging applications, *e.g.*, gold, silver.¹⁷⁻²¹ The peptide coating greatly increases the colloidal stability and biocompatibility of noble metal nanoparticles and prevents any major problems encountered during biological applications, *e.g.*, electrolyte-induced aggregation, ligand exchange, non-specific binding to biomolecules or cell membranes, and cell toxicity. Furthermore, the peptide coating offers the possibility to functionalize the nanoparticles with stoichiometric control with targeting moieties, *e.g.*, peptides, proteins, *via* either affinity or covalent conjugation. Recently, we demonstrated the use of peptide coated gold nanoparticles to probe specific cell targets²² and to enable their specific internalization

into confined areas, *i.e.*, porous protein cages cores,²³ which are otherwise not possible with bulky nanomaterials.

Herein, we report the design of a library of short peptides and ligands to create biocompatible peptide coated USPIOs for *in vivo* contrast-enhanced MRI applications. A total of 86 different peptide coated USPIOs were prepared and we identified the highest performing candidates *via* a stringent selection process, *e.g.*, size mono-dispersity, long-term stability in physiological conditions, cytotoxicity and cell non-specific binding, *in vitro* and *in vivo* magnetic resonance performances. We demonstrated the greater stability of bis-phosphorylated anchor groups located at the foot of peptides and ligands, compared to mono-phosphorylated groups or other moieties commonly used for the coating of iron oxide nanomaterials, *e.g.*, L-3,4-dihydroxyphenylalanine (DOPA).²⁴ Specifically, the bis-phosphorylated peptide 2PG-S*VVVT-PEG4-ol and the mixed peptide ligand 2PG-S*VVVT-ol:(PO₃H₂)-S-C11-EG3-OH (70:30, mole:mole) coated USPIOs had the highest stability and biocompatibility over a long time *in vitro*. Importantly, they also outperformed the magnetic resonance properties of commercially available contrast agents, *i.e.*, Magnevist® and Resovist®, with greater relaxivities and r₂/r₁ ratios, which indicates their utility for T2-weighted MRI applications. Most interestingly, we demonstrated the high contrast enhancement provided by the 2PG-S*VVVT-PEG4-ol coated USPIOs during T2-weighted MRI in liver *in vivo* and their application for the detection of liver tumors. This investigation will enable further development of the peptide coated USPIOs, such as biofunctionalization with biomarkers, for the utilization of peptide coated USPIOs for the early detection of other types of tumors and diseases by MRI.

RESULTS AND DISCUSSION

Method for the preparation and selection of peptide coated USPIOs for *in vivo* contrast-enhanced MRI. In this investigation, we prepared and selected highly stable and biocompatible peptide coated USPIOs with the best performance as T2 contrast agents for *in vivo* MRI applications (Figure 1).

In a first step (Figure 1a), the phase transfer of oleic acid coated USPIOs dispersed in chloroform to an aqueous phase was carried out by ligand exchange of the oleic acid coating with tetramethylammonium

hydroxide (TMAOH). We designed a library of 20 short peptides and ligands and tested their ability to form a stable SAM on the USPIOs surface *via* direct ligand exchange of the preliminary TMAOH coating (Figure 1b). We prepared 86 single and mixed peptide coated USPIOs and evaluated them following a “funnel selection process” in which a series of increasingly stringent tests were used to select the most performing peptide coated USPIOs contrast agents for *in vivo* contrast-enhanced MRI applications (Figure 1c). We evaluated each peptide coating for its ability to protect the surface of USPIOs and allow purification by size-exclusion chromatography (SEC), stabilize USPIOs against electrolyte-induced aggregation in physiological conditions, prevent non-specific binding to live cells, present no cell toxicity and provide strong magnetic resonance properties *in vitro* and enhanced contrast during *in vivo* MRI. We evaluated the most performing peptide coated USPIOs against commercial MRI contrast agents used in the clinic, Resovist®, Magnevist®.

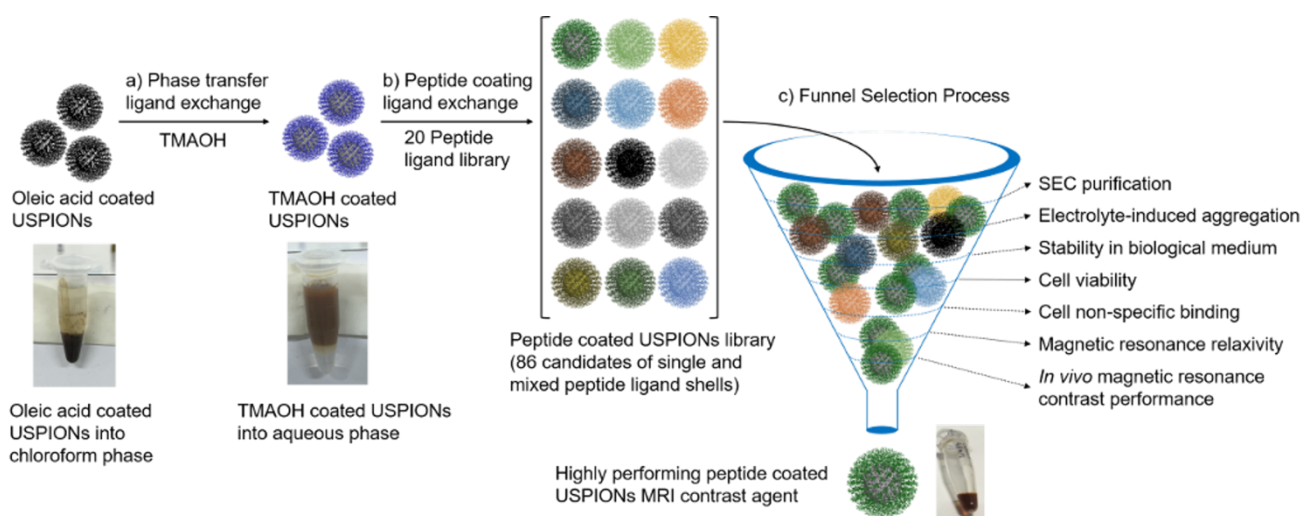


Figure 1. Method for the preparation and selection of high-performing peptide coated USPIOs MRI contrast agents. a) Phase transfer of oleic acid coated USPIOs dispersed in chloroform to aqueous phase by ligand exchange with tetramethylammonium hydroxide (TMAOH); b) Peptide coating of water-dispersed TMAOH coated USPIOs by ligand exchange reaction. A library of 86 candidates of single and mixed peptide ligand coated USPIOs was prepared and evaluated; c) Funnel selection process for the determination of the most performing peptide coated USPIOs contrast agent for *in vivo* contrast-enhanced MRI.

Tailored peptide library. We designed a library of 20 short peptides and ligands to form stable SAMs on the surface of USPIONs (Table 1). The tailoring of peptides that will form SAMs on the surface of nanoparticles follows three common features: 1) a foot, to anchor the peptides onto the nanoparticle surface; 2) a stem, to favor peptide-peptide interactions and increase the SAM packing density, and; 3) a head, to improve the colloidal stability and prevent non-specific interactions with the biological environment.^{17,18,20,21} Each feature ensures then the formation of highly stable and biocompatible peptide coated USPIONs.

Table 1. Peptide and ligand library design.

| Alkyl phosphorothioic acid ligands | Ligands bearing phosphorylated amino acid anchor groups | | Peptides bearing phosphorylated amino acid anchor groups | | Peptide ligands bearing non-phosphorylated anchor groups |
|--|---|--------------------|--|--------------------|--|
| | Single phosphate | Double phosphate | Single phosphate | Double phosphate | |
| (PO ₃ H ₂)-S-C11-EG3-OH | H-S*-NH-PEG4-ol | 2PG-S*-C11-PEG4-ol | H-S*SSSS-ol | 2PG-S*VVVT-ol | N(Me)-C11-PEG4-ol |
| (PO ₃ H ₂)-S-C11-EG6-OH | 2PG-NH-PEG4-ol | | H-S*PPPT-ol | 2PG-Y*VVVT-ol | H-DVVVT-ol |
| (PO ₃ H ₂)-S-C16-OH | 2PG-G-NH-PEG4-OH | | H-S*VVVT-ol | 2PG-S*VVVT-PEG4-ol | DOPA-VVVT-ol |
| | 2PG-G-NH-PEG4-ol | | | | DOPA-VVVT-PEG4-ol |
| | H-S*-C11-PEG4-ol | | | | DOPA-C11-PEG4-ol |

^a The letter S is a sulfur atom in this case.

Abbreviations: 2PG = (PO₃H₂)-O-CH₂-CO-, 2-phosphoglycolic acid; S* and Y* = Ser(PO₃H₂) and Tyr(PO₃H₂) respectively; EG3-OH = -(O-CH₂-CH₂)₃-OH; EG6-OH = -(O-CH₂-CH₂)₆-OH; PEG4-ol = -NH-(CH₂-CH₂-O)₃-CH₂-CH₂-OH; PEG4-OH = -NH-(CH₂-CH₂-O)₄-CH₂-CH₂-CO₂H; C11 = -(CH₂)₁₁-; C16 = -(CH₂)₁₆-; DOPA = L-3,4-dihydroxyphenylalanine.

The foot of the peptide is essential to increase the SAM stability and limit peptide loss from the nanoparticle surface, in particular from ligand exchange reactions with small biomolecules present in the biological environment. Phosphate and phosphonic acid groups have a strong affinity to metals and metal oxides such as iron oxide surfaces.^{25,26} In particular, the robustness of the chemical bond formed between the surface of iron oxide nanoparticles and phosphorylated groups helped develop affinity chromatography techniques for the purification of phosphorylated peptides and protein digests of biological interest.²⁷ Inexpensive protein lysates containing phosphorylated peptides such as Tryptone were also proposed to encapsulate iron oxide nanoparticles.²⁸ However, although the preparation of peptide coated iron oxide nanoparticles from protein lysates is an attractive solution, their polydispersity and

quasi-random amino acid sequences limits the stability of the nanoparticles coating. Here, we designed peptides and ligands with a single or bis-phosphorylated foot using phosphorylated moieties such as phosphorothioic, phosphorylated amino acids (Ser(PO₃H₂) and Tyr(PO₃H₂)) and 2-phosphoglycolic acid (2PG). We also compared the stability of phosphorylated peptide SAMs with peptides and ligands presenting other anchor groups used for iron oxide surfaces, *i.e.*, quaternary amine, carboxylic acid and L-3,4-dihydroxyphenylalanine (DOPA).²⁴

Peptides and ligands with a short stem such as pentapeptides and short alkane chains form highly stable and dense SAMs on noble metal nanoparticles.^{17,18,20-23} Non-charged and non-polar stems also favor van der Waals interactions between peptides and ligands and increase the packing density of SAMs. Therefore we used pentapeptide sequences, *e.g.*, -SVVVT-, -SSSSS- and -SPPPT-, and alkane chains, *e.g.*, undecane and hexadecane.¹⁸

We also used hydrophilic and non-charged moieties to form the heads of the peptides and ligands, *e.g.*, alcohol and ethylene glycol. The hydrophilic property of the peptide head improves the water-dispersion of nanoparticles and ethylene glycol groups increase steric repulsion and colloidal stability, limiting non-specific binding to biomaterials, *e.g.*, proteins and cell membranes. Alternatively, charged moieties such as carboxylic acids may also improve colloidal stability, *e.g.*, H-CALNN-OH peptide coated gold nanoparticles.²¹ However, the increased non-specific interactions with biomolecules presenting opposite charges is a major inconvenience to charged nanoparticle surfaces. Hence, we only included a single instance of carboxylic acid terminated ligand (2PG-G-NH-PEG4-OH) in our library for comparison.

Preparation and characterization of water soluble TMAOH coated USPIONs. We mixed oleic acid coated USPIONs dispersed in chloroform with an aqueous solution of tetramethylammonium hydroxide (TMAOH) to replace the hydrophobic coating with a hydrophilic TMAOH one and so phase transfer TMAOH coated USPIONs into water. Electron microscopy analysis showed the conservation of the size of the USPIONs' core, with an average size of 11.3 ± 1.3 nm in diameter of the oleic acid coated USPIONs (Figure 2A) and an average size of 10.1 ± 0.9 nm in diameter of the TMAOH coated USPIONs (Figure 2B). The crystal structure of the USPIONs core corresponding to gamma-Fe₂O₃ iron oxide (maghemite)

was also conserved after phase transfer as shown by X-ray powder diffraction analysis (Figures 2C,D) and high-resolution electron microscopy (Figure 2E). The dynamic light scattering analysis of TMAOH coated USPIONs showed a hydrodynamic size of 10 ± 3 nm (Figure 2F and Table 2) and a zeta potential of -50 ± 1 mV (Table 2).

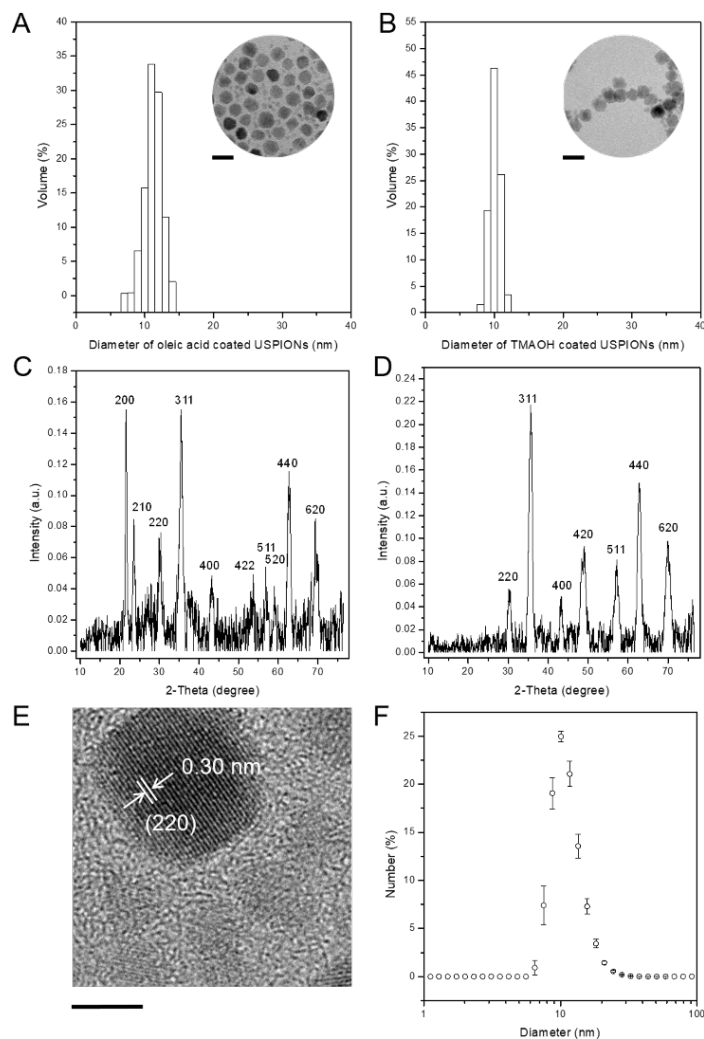


Figure 2. Characterization of oleic acid coated USPIONs and water soluble TMAOH coated USPIONs. Size distribution by electron microscopy analysis of (A) 100 oleic acid coated USPIONs with average diameter of 11.3 ± 1.3 nm and (B) 100 TMAOH coated USPIONs with average diameter of 10.1 ± 0.9 nm. Insets show typical images used for calculations. Scale bar is 20 nm. X-ray powder diffraction of (C) oleic acid coated USPIONs and (D) TMAOH coated USPIONs with 2-Theta peaks corresponding to gamma-Fe₂O₃ iron oxide, maghemite (cubic) crystal structure. (E) High-resolution electron microscopy

picture of oleic acid coated USPIONs with single crystallinity and lattice fringes across the entire nanoparticles corresponding to $\text{Fe}_2\text{O}_3(220)$. Scale bar is 5 nm. (F) Dynamic light scattering characterization of 10 ± 3 nm TMAOH coated USPIONs ($\text{Pdi} = 0.262$).

Preparation and purification of peptide coated USPIONs. We evaluated first the ability of each peptide and ligand from our library to stabilize USPIONs. The ligand exchange reaction of the TMAOH coating onto USPIONs surface with peptides and ligands was adapted from our previous work on the preparation of peptide coated gold nanoparticles from citrate coated gold nanoparticles,⁸ and the preparation of peptide coated magnetic iron oxide nanoparticles (IONPs) from TMAOH coated IONPs reported by Barch *et al.*.²⁹ Firstly, 0.1 volume of TMAOH coated USPIONs dispersed in 0.1% (w/v) TMAOH aqueous solution were diluted with 8.9 volumes of water and mixed with 1 volume of a 2 M peptide or ligand solution for an hour. This step allowed for an initial ligand exchange reaction of the weak TMAOH coating with peptides and ligands bearing anchor groups that strongly bond to iron oxide surfaces, *e.g.*, *via* phosphate and phosphonic acid. Secondly, the samples were mixed with 1 volume of 200 mM HEPES, 1 M NaCl (pH 7.4) at room temperature overnight.

We noted here that the stability of the peptide coated USPIONs in a relatively high concentration of NaCl (100 mM) present in the HEPES buffer indicated that a rapid initial ligand exchange of the TMAOH coating occurred in the first step, since TMAOH coated USPIONs were not stable in presence of NaCl. The peptide coated USPIONs were then purified by size-exclusion chromatography (SEC) on Sephadex G25 resin to remove the excess of peptides and ligands. Sephadex G25 is a cross-linked dextran, so SEC also evaluated the potential for non-specific binding to biomaterials, *e.g.*, polysaccharides. We determined the yield of the preparation of each peptide coated USPIONs after SEC purification by UV-visible spectrometry and their hydrodynamic size and zeta potential by DLS (Table 2, Figure S1).

Table 2. Size-exclusion chromatography of single peptide coated USPIONs and characterization of zeta potentials and hydrodynamic sizes by dynamic light scattering.

| Peptide ligand design | Yield after SEC purification (%) | DLS size (nm) | Zeta potential (mV) |
|--|----------------------------------|---------------|---------------------|
| TMAOH | 0 | 10 ± 3 | -50 ± 1 |
| (PO ₃ H ₂)-S-C11-EG3-OH | 0 | - | - |
| (PO ₃ H ₂)-S-C11-EG6-OH | 0 | - | - |
| (PO ₃ H ₂)-S-C16-OH | 86 ± 7 | 59 ± 34 | -37 ± 1 |
| H-S*-NH-PEG4-ol | 0 | - | - |
| 2PG-NH-PEG4-ol | 0 | - | - |
| 2PG-G-NH-PEG4-OH | 0 | - | - |
| 2PG-G-NH-PEG4-ol | 0 | - | - |
| H-S*-C11-PEG4-ol | 0 | - | - |
| 2PG-S*-C11-PEG4-ol | 88 ± 4 | 51 ± 19 | -17 ± 1 |
| H-S*SSSS-ol | 0 | - | - |
| H-S*PPPT-ol | 0 | - | - |
| H-S*VVVT-ol | 0 | - | - |
| 2PG-S*VVVT-ol | 85 ± 10 | 18 ± 7 | -16 ± 2 |
| 2PG-Y*VVVT-ol | 69 ± 6 | 33 ± 16 | -28 ± 1 |
| 2PG-S*VVVT-PEG4-ol | 94 ± 4 | 18 ± 8 | -14 ± 2 |
| N(Me)-C11-PEG4-ol | 0 | - | - |
| H-DVVVT-ol | 0 | - | - |
| DOPA-VVVT-ol | 0 | - | - |
| DOPA-VVVT-PEG4-ol | 34 ± 3 | 51 ± 23 | -11 ± 1 |
| DOPA-C11-PEG4-ol | 0 | - | - |

Data were acquired on duplicate from two experiments and presented as average and standard deviation.

The mono-phosphorylated ligand (PO₃H₂)-S-C16-OH, the bis-phosphorylated ligand 2PG-S*-C11-PEG4-ol and the bis-phosphorylated peptides 2PG-S*VVVT-ol and 2PG-S*VVVT-PEG4-ol stabilized the USPIONs with high yields (>80%). DLS analysis showed that only the two bis-phosphorylated peptides 2PG-S*VVVT-ol and 2PG-S*VVVT-PEG4-ol formed coatings with minimal hydrodynamic size increase (18 nm) (Table 2). We suggest that a significant increase of the peptide coated USPIONs hydrodynamic size indicated the formation of less organized and stable surface coatings rather than a compact SAM. The hypothesis was supported with the zeta potential of 2PG-S*VVVT-ol and 2PG-S*VVVT-PEG4-ol coated USPIONs being the closest to neutral, *i.e.*, -16 and -14 mV respectively. Considering the neutral heads of the peptides and ligands exposed at the surface of the USPIONs coatings

and the negative zeta potential of the initial TMAOH coated USPIONs (-50 mV), this result confirmed a greater coverage of the USPIONs surface than for peptide or ligand coated USPIONs with more negative zeta potentials (Table 2).

Despite the similarity of the design of some peptides and ligands, we observed that specific features were necessary to form stable peptide coating on USPIONs (Table 2). For instance, the comparison of peptides with different foot design, *i.e.*, 2PG-S*VVVT-ol, H-S*VVVT-ol, H-DVVVT-ol, DOPA-VVVT-ol, indicated that a bis-phosphorylated anchor group provided greater stability to the peptide coating than other groups that are also known to have good affinity to iron oxide surface, *e.g.*, mono-phosphorylated groups, carboxylic acid, DOPA. The same trends were observed with ligands designed with undecane stems and ethylene glycol heads, *i.e.*, 2PG-S*-C11-PEG4-ol, H-S*-C11-PEG4-ol, (PO₃H₂)-S-C11-EG3-OH, N(Me₂)-C11-PEG4-ol and DOPA-C11-PEG4-ol. In the latter case, only bis-phosphorylated anchor groups provided sufficient stability to USPIONs. We also observed that ligands without a stem, *i.e.*, H-S*-NH-PEG4-ol, 2PG-NH-PEG4-ol, 2PG-G-NH-PEG4-OH and 2PG-G-NH-PEG4-ol, did not provide sufficient stability to USPIONs and indicated that a stem is required.

Following the first screening of single peptide coated USPIONs, we prepared mixed ligand coated USPIONs with binary combinations of a peptide and a ligand from our library. As demonstrated in our previous studies,^{18,20} the combination of short peptidols and alkane ethylene glycol ligands provides highly stable mixed peptide coatings on metal nanoparticles. Ethylene glycol groups at the head position of ligands present sufficient flexibility and steric repulsion on the surface of the nanoparticles to increase their colloidal stability. Moreover, the neutral alcohol groups at the carboxyl-terminal position of the peptidols and the alkane ethylene glycol ligands help prevent from non-specific binding to charged molecules. We found that a SAM called Mix-matrix formed with a mixture of the pentapeptidol H-CVVVT-ol and a short thiolated undecane ethylene glycol ligands HS-C11-EG4 provided great stability to gold¹⁸ and silver nanoparticles.¹⁷ Similarly, here we selected from our library 8 peptides, *i.e.*, H-S*SSSS-ol, H-S*PPPT-ol, H-S*VVVT-ol, 2PG-S*VVVT-ol, 2PG-Y*VVVT-ol, 2PG-S*VVVT-PEG4-ol, DOPA-VVVT-ol and DOPA-VVVT-PEG4-ol, and 5 ligands, *i.e.*, (PO₃H₂)-S-C11-EG3-OH, (PO₃H₂)-S-

C11-EG6-OH, (PO₃H₂)-S-C16-OH, 2PG-S*-C11-PEG4-ol and DOPA-C11-PEG4-ol. We prepared mixed peptide coated USPIONs with peptide to ligand molar ratios of 70:30, 50:50 and 30:70 (all mole:mole). The yields of the preparation of the mixed peptide coated USPIONs were determined by UV-visible spectrometry after SEC purification, and the hydrodynamic sizes and zeta potentials characterized by DLS (Table S1). A summary of the successful purifications by SEC of the mixed peptide coated USPIONs is presented in Table 3.

Table 3. Qualitative summary of size-exclusion chromatography of mixed peptide coated USPIONs.

| | (PO ₃ H ₂)-S-C11-EG3-OH | | | (PO ₃ H ₂)-S-C11-EG6-OH | | | (PO ₃ H ₂)-S-C16-OH | | | 2PG-S*-C11-PEG4-ol | | | DOPA-C11-PEG4-ol | | |
|--------------------------------------|--|-------|-------|--|-------|-------|--|-------|-------|--------------------|-------|-------|------------------|-------|-------|
| | 70:30 | 50:50 | 30:70 | 70:30 | 50:50 | 30:70 | 70:30 | 50:50 | 30:70 | 70:30 | 50:50 | 30:70 | 70:30 | 50:50 | 30:70 |
| Peptide to ligand (mole:mole) | | | | | | | | | | | | | | | |
| H-S*SSSS-ol | - | - | - | - | - | - | + | + | + | | | | | | |
| H-S*PPPT-ol | - | - | - | - | - | - | + | + | + | | | | | | |
| H-S*VVVT-ol | - | - | - | - | - | - | + | + | + | | | | | | |
| 2PG-S*VVVT-ol | + | + | + | + | + | + | + | + | + | + | + | + | | | |
| 2PG-Y*VVVT-ol | + | - | - | + | - | - | + | + | + | + | + | + | | | |
| 2PG-S*VVVT-PEG4-ol | + | + | + | + | + | + | + | + | + | | | | | | |
| DOPA-VVVT-ol | | | | | | | | | | | | | - | - | - |
| DOPA-VVVT-PEG4-ol | | | | | | | | | | | | | - | - | - |

A sign (+) indicates the successful purification of the peptide coated USPIONs by SEC, allowing to collect sufficient USPIONs for DLS and zeta potential characterization. A sign (-) indicates that no peptide coated USPIONs were collected after SEC. The full dataset is presented in Table S1.

We observed first that the ligand (PO₃H₂)-S-C16-OH was successful when mixed with a mono-phosphorylated peptide. The mixed peptide coated USPIONs prepared with the bis-phosphorylated peptides, *i.e.*, 2PG-S*VVVT-ol, 2PG-Y*VVVT-ol, 2PG-S*VVVT-PEG4-ol, had generally higher preparation yields, regardless of the second ligand type or the molar ratio. DOPA functionalized peptides and ligands were not able to stabilize the USPIONs even though the design of the stems and heads of the peptides and ligands were identical to other combinations stabilizing the USPIONs, *e.g.*, 2PG-S*VVVT-ol and (PO₃H₂)-S-C16-OH. Therefore, phosphorylated anchor groups at the foot of peptides and ligands improved the stability of USPIONs. For most mixed peptide coated USPIONs, hydrodynamic sizes zeta

potentials were consistent with the results from single peptide coated USPIONs, as we observed with low increases in the hydrodynamic radius, *e.g.*, 18 nm, and large increase of the zeta potential after ligand exchange, *e.g.*, -20 mV (Table S1).

Stability of peptide coated USPIONs against electrolyte-induced aggregation. We evaluated the stability of the peptide coated USPIONs that largely did not bind to Sephadex G25 against electrolyte-induced aggregation in physiological conditions and in high electrolyte concentrations to identify the most performing peptide coated USPIONs for *in vitro* and *in vivo* applications. Similarly to our previous studies on the preparation of biocompatible peptide coated gold nanoparticles,^{18,20} we used a normalized aggregation parameter (NAP) based on the comparison of the UV absorption of each USPIONs preparation before and after incubation in various conditions, *i.e.*, NaCl concentrations from 0 to 1 M, buffers (HEPES, PBS), at room temperature or 37°C, and incubation times (up to 48 h).

The evaluation of single peptide coated USPIONs revealed distinct differences in stability depending on the design of the peptide and ligand (Figure 3A-C). The detailed results obtained are available in supplementary information (Figures S2-S7). After 3 h incubation in 20 mM HEPES at pH 7.4 in NaCl concentrations ranging from 0 to 1 M at room temperature (Figure 3A) the bis-phosphorylated peptidols 2PG-S*VVVT-ol and 2PG-Y*VVVT-ol coated USPIONs were the least stable and aggregated. We noted also that the differences in hydrodynamic sizes and zeta potentials (Table 2) between the two peptidol coated USPIONs were not reliable indicators of stability towards electrolyte-induced aggregation. Moreover, this result correlated with our previous studies with similar single peptide coated gold nanoparticles, *e.g.*, H-CVVVT-ol,¹⁸ which showed that a peptidol alone is not able to stabilize efficiently metal nanoparticles and needs an additional ligand to form a stable SAM, *e.g.*, Mix-matrix coated gold nanoparticles with the peptidol H-CVVVT-ol and the ligand HS-C11-EG4. Surprisingly, the mono-phosphorylated ligand (PO₃H₂)-S-C16-OH demonstrated greater stability than the bis-phosphorylated ligand 2PG-S*-C11-PEG4-ol, even though the former possess only a single phosphorylation anchor group and lacks an ethylene glycol moiety often necessary to reduce electrolyte-induced aggregation, *e.g.*, HS-C11-EG4 coated gold nanoparticles.¹⁸ Most importantly, the bis-phosphorylated peptide 2PG-S*VVVT-

PEG4-ol provided the greatest stability in all incubation conditions (Figure 3A-C) and showed no sign of aggregation after long incubation time even in high NaCl concentrations (1 M) and at 37°C. Interestingly too, the 2PG-S*VVVT-PEG4-ol coated USPIONs were purified with the greatest yield (>94%) and showed the lowest increase of hydrodynamic size (18 nm) and a large increase of zeta potential (-14 mV) (Table 2). Hence, the presence of a short hydrophilic ethylene glycol at the head of the peptide 2PG-S*VVVT-PEG4-ol provided sufficient steric hindrance at the surface of the USPIONs to prevent electrolyte-induced aggregation. A similar peptide design, *i.e.*, DOPA-VVVT-PEG4-ol, also demonstrated promising results in high electrolyte concentrations and after long incubation times in 20 mM HEPES at room temperature (Figure 3B). However, it failed to remain stable at 37°C (Figure 3C).

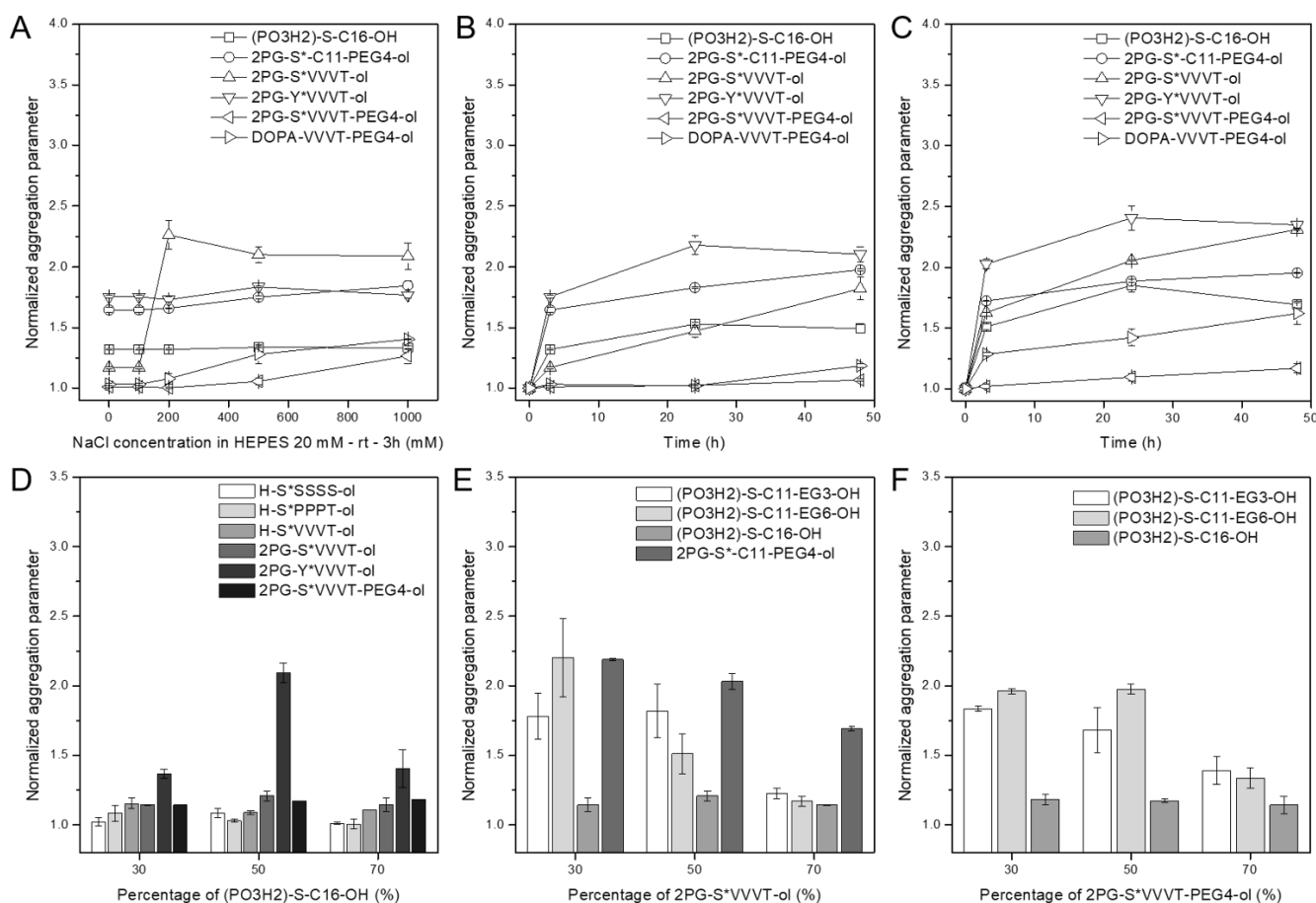


Figure 3. Stability of peptide coated USPIONs against electrolyte-induced aggregation. Normalized aggregation parameter values of single peptide coated USPIONs: (A) after 3 h incubation at room temperature in a 20 mM HEPES buffer (pH 7.4) and a range of concentrations of NaCl; after different incubation

times in 20 mM HEPES and 100 mM NaCl buffer (pH 7.4) at (B) room temperature and (C) 37°C. Normalized aggregation parameter values of selected mixed peptide coated USPIONs incubated for 24 h in 20 mM HEPES and 100 mM NaCl buffer (pH 7.4) at room temperature. Mixed peptide coated USPIONs formed with: (D) different peptides and the ligand (PO₃H₂)-S-C16-OH; (E) different ligands and the peptidol 2PG-S*VVVT-ol; (F) different ligands and the peptide 2PG-S*VVVT-PEG4-ol, at different molar ratios. Data were acquired on duplicate from two experiments and presented as average and standard deviation.

The stability of mixed peptide coated USPIONs against electrolyte-induced aggregation was then evaluated. The detailed results are available in supplementary information (Figures S8-S45). The normalized aggregation parameter values of selected mixed peptide coated USPIONs incubated for 24 h in 20 mM HEPES buffer at pH 7.4 at room temperature are presented in Figures 3D-F. Mixed peptide coatings prepared with a mono or bis-phosphorylated peptide combined with the ligand (PO₃H₂)-S-C16-OH (Figure 3D) were in most instances stable. Interestingly, although the mono-phosphorylated peptidols H-S*SSSS-ol, H-S*PPPT-ol and H-S*VVVT-ol did not form stable single peptide coated USPIONs, they were relatively stable when mixed with the ligand (PO₃H₂)-S-C16-OH. Mixed peptide coated USPIONs formed with the peptidols H-S*SSSS-ol, H-S*PPPT-ol or H-S*VVVT-ol and mixed with the ligand (PO₃H₂)-S-C16-OH were among the most stable, however this result was not directly correlated to the preparation yields (Table S1) that were in most cases lower. Most mixed peptide coated USPIONs formed with the ligand (PO₃H₂)-S-C16-OH had a relatively low hydrodynamic size (~ 20 nm) and close to neutral zeta potential (~ -15 mV) (Table S1), which indicated the formation of a dense SAM on the USPIONs' surface. Mixed peptide coated USPIONs formed with the mono-phosphorylated peptidol 2PG-S*VVVT-ol or the bis-phosphorylated peptide 2PG-S*VVVT-PEG4-ol were similarly affected by the ligand used and were most stable with the ligand (PO₃H₂)-S-C16-OH (Figures 3E,F). The ethylene glycol moiety on the peptide

2PG-S*VVVT-PEG4-ol did not affect the stability of mixed peptide coated USPIONs. Overall, the combination of the peptidol 2PG-S*VVVT-ol and the ligand (PO₃H₂)-S-C16-OH provided the greatest performance for mixed peptide coated USPIONs.

Cell toxicity and non-specific binding. Two highly stable USPIONs preparations were selected for further *in vitro* evaluation: the single peptide 2PG-S*VVVT-PEG4-ol and the mixed peptide 2PG-S*VVVT-ol:(PO₃H₂)-S-C11-EG3-OH (70:30, mole:mole) coated USPIONs. We evaluated the cell toxicity of the two preparations *in vitro* with PLC/PRF5 cells. We measured cell growth using a CellTiter 96® AQueous One Solution Cell Proliferation Assay (MTS). We observed no toxicity compared to a control (untreated cells) after 2 days incubation at 37°C with either 2PG-S*VVVT-PEG4-ol or 2PG-S*VVVT-ol:(PO₃H₂)-S-C11-EG3-OH (70:30, mole:mole) coated USPIONs at 100 μg/mL of Fe (Figure 4A,B). We also tested the non-specific binding of both preparations after overnight incubation at 37°C with PLC/PRF5 cells. Cell staining with Prussian blue reagent showed no detectable non-specific binding for either peptide coated USPIONs preparation at 10 μg/mL and at 100 μg/mL of Fe (Figure 4F,G). However, the slight increase of the cell viability observed at the highest concentration, *i.e.*, 100 μg/mL, may be due to the potential presence of peptide coated USPIONs non-specifically bound to the cells and contributing to the absorbance of the samples at 490 nm, which is the readout of the cytotoxicity assay (Figures 4A,B). Alternatively, the low level of cell-associated USPIONs (not detected by the Prussian blue assay), may trigger a cellular response that increases mitochondrial membrane potential, and hence MTT assay signal. In any event, these USPIONs are not cytotoxic.

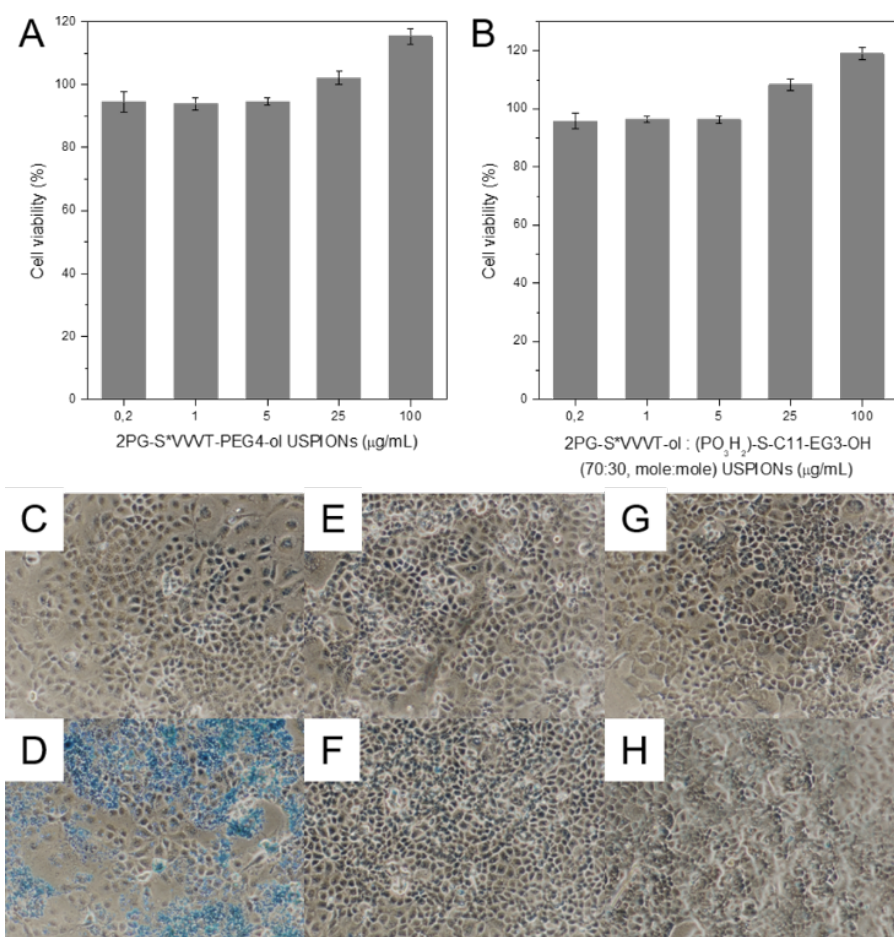


Figure 4. *In vitro* evaluation of peptide coated USPIONs. Cell viability assay of selected peptide coated USPIONs with PLC/PRF5 cells: **(A)** 2PG-S*VVVT-PEG4-ol and **(B)** 2PG-S*VVVT-ol:(PO₃H₂)-S-C11-EG3-OH (70:30, mole:mole) coated USPIONs showed no cell toxicity at the test concentration of 100 µg/mL of Fe after 48 h of incubation at 37°C. Cell non-specific binding test of peptide coated USPIONs with PLC/PRF5 cells. **(C)** Control sample showing PLC/PRF5 cells incubated without USPIONs. Cells were incubated overnight at 37°C with **(D)** TMAOH coated USPIONs, **(E-F)** 2PG-S*VVVT-PEG4-ol and **(G-H)** 2PG-S*VVVT-ol: (PO₃H₂)-S-C11-EG3-OH (70:30, mole:mole) coated USPIONs at the test concentration of 10 µg/mL **(E,G)** and 100 µg/mL **(D,F,H)** of Fe. Cells were stained with Prussian blue reagent and counterstained with Nuclear Fast Red solution. All experiments were repeated three times and presented as average and standard deviation.

Magnetic relaxation performance. The magnetic resonance relaxivities r_1 and r_2 of 2PG-S*VVVT-PEG4-ol and 2PG-S*VVVT-ol:(PO₃H₂)-S-C11-EG3-OH (70:30, mole:mole) coated USPIOs were characterized with a 7T magnetic resonance imaging system (Table 4 and Figures S46-49). We also compared their performance to the commercial MRI contrast agents Magnevist® and Resovist®. 2PG-S*VVVT-PEG4-ol and 2PG-S*VVVT-ol:(PO₃H₂)-S-C11-EG3-OH (70:30, mole:mole) coated USPIOs presented high transverse relaxivity coefficients (r_2), *i.e.*, 217.8 and 173.9 mM⁻¹.s⁻¹ respectively. Importantly, r_2/r_1 ratios define the quality of MRI contrast agents dedicated to either T1 or T2-weighted imaging.³⁰ The r_2/r_1 ratio of T1 contrast agent Magnevist® was close to 1. Typically, T2 contrast agents such as Resovist® have higher r_2/r_1 ratios. The peptide coated USPIOs demonstrated greater r_2/r_1 ratios than the commercial T2 contrast agent Resovist® ($r_2/r_1 = 69.4$), *i.e.*, 90.8 and 108.7 for 2PG-S*VVVT-PEG4-ol and 2PG-S*VVVT-ol:(PO₃H₂)-S-C11-EG3-OH (70:30, mol:mol) coated USPIOs respectively.

Table 4. Longitudinal and transverse relaxivities of commercial magnetic resonance imaging contrast agents and peptide coated USPIOs.

| Peptide coated USPIOs / Commercial contrast agents | r_1 (mM ⁻¹ .s ⁻¹) | r_2 (mM ⁻¹ .s ⁻¹) | r_2/r_1 ratios |
|--|--|--|------------------|
| Magnevist® | 3.8 | 6.2 | 1.6 |
| Resovist® | 3.5 | 242.9 | 69.4 |
| 2PG-S*VVVT-ol: (PO ₃ H ₂)-S-C11-EG3-OH (70:30, mol:mol) | 1.6 | 173.9 | 108.7 |
| 2PG-S*VVVT-PEG4-ol | 2.4 | 217.8 | 90.8 |

***In vivo* liver and tumor magnetic resonance imaging.** We next tested the performance of 2PG-S*VVVT-PEG4-ol coated USPIOs *in vivo* contrast-enhanced T2-weighted MRI in NCr nude mice using a 7T Bruker Clinscan. Intramuscular contrast enhancement was first evaluated using a 10 mg Fe per kg of mouse body weight injection of the peptide coated USPIOs in the hind limb. Images confirmed a strong 80% decrease of the MRI signal (Figure S50). Iron oxide nanoparticles contrast agents have been for long proposed and approved for clinical contrast-enhanced T2-weighted MRI of the liver, because they are promptly engulfed by Kupffer cells and macrophages prior to storage and metabolism in the liver.³¹ We injected intravenously a dose of 1.0 mg Fe per kg of 2PG-S*VVVT-PEG4-ol coated USPIOs

into NCr nude mice. As anticipated, we observed a strong and persistent decrease of the signal ($48 \pm 4 \%$ at 0.5 h and $52 \pm 7 \%$ at 1 h) in the liver during T2-weighted MRI (Figure 5A,B). The application of USPIOs as contrast agents has been extended to the imaging of liver lesions, such as those associated with cirrhosis and tumors, using T2-weighted MRI to obtain pseudo positive contrast signals, because of the differences in vascularity and Kupffer cell activity of affected and healthy liver tissues.^{31,32} To evaluate the use of our peptide coated USPIOs for the imaging of liver tumors, we performed a T2-weighted MRI on an orthotopic liver tumor model established by inoculation of PLC/PRF5 cells into the liver of nude mice. Once the tumors reached 5 mm, we injected intravenously the 2PG-S*VVVT-PEG4-ol coated USPIOs at a dose of 20 mg of Fe per kg and monitored the contrast-to-noise (CNR) ratios of tumor-to-liver contrast enhancement provided by USPIOs. We found a significant CNR gain at 1 h ($28 \pm 8 \%$) and enhancement of the definition of the liver tumors contour (Figures 5C,D). Histopathological analysis showed the presence of the peptide coated USPIOs in the liver of mice after 1 h post injection (Figures 5E,F). Interestingly, the presence of the peptide coated USPIOs in healthy liver tissues was clearly confirmed (Figure 5E - high right region, and Figure 5F) and we noted the absence of peptide coated USPIOs in the tumor region of the liver (Figure 5E - low left region). The utilization of the peptide coated USPIOs may, therefore, contribute to the imaging of early liver cancer lesions by MRI.

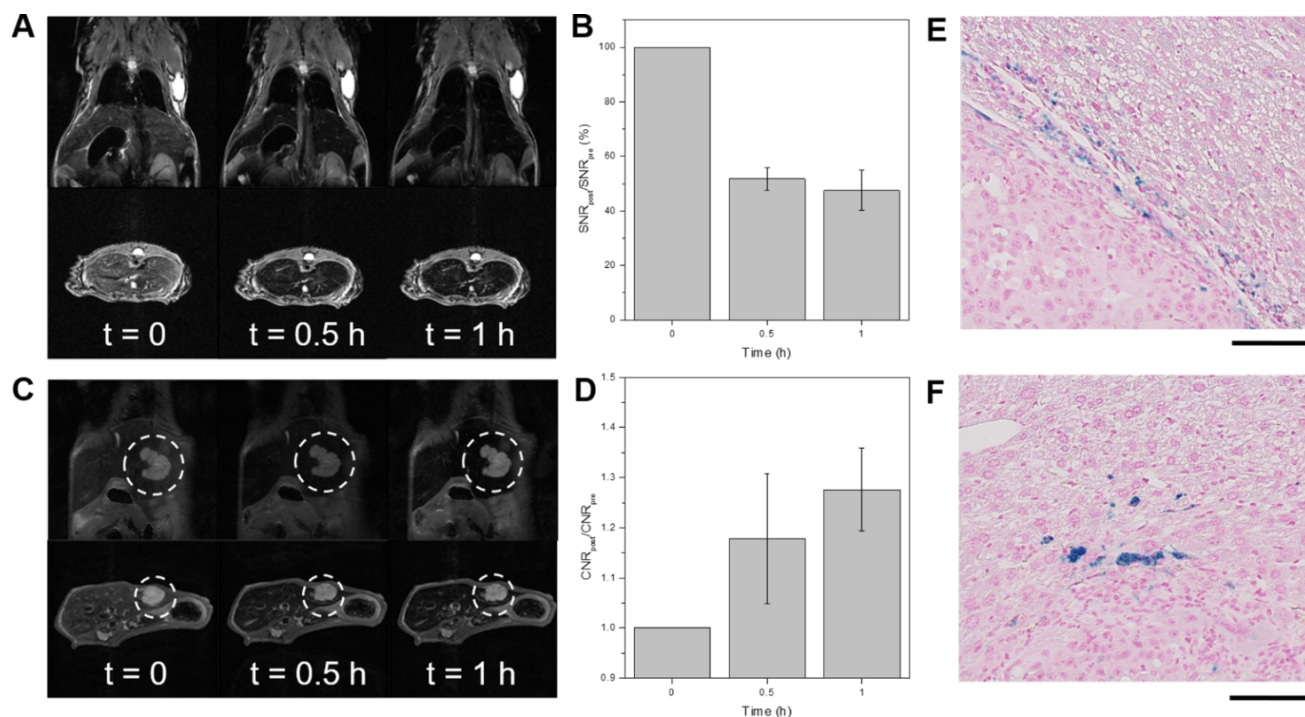


Figure 5. *In vivo* MRI with the 2PG-S*VVVT-PEG4-ol coated USPIOs contrast agent. **(A)** *In vivo* MR images in coronal (upper) and transverse (lower) plane of NCr nude mouse at 0, 0.5 and 1 h after intravenous injection of 2PG-S*VVVT-PEG4-ol coated USPIOs. **(B)** Quantification of liver contrast collected at 0, 0.5 and 1 h after accumulation of peptide coated USPIOs in NCr nude mice at dose of 1.0 mg Fe per kg. **(C)** *In vivo* MR images in coronal (upper) and transverse (lower) plane of orthotopic xenograft liver tumor model at 0, 0.5 and 1 h after intravenous injection of 2PG-S*VVVT-PEG4-ol coated USPIOs. Dashed circle indicates the tumor location. **(D)** Quantification of contrast-to-noise ratio (CNR) of tumor-to-liver contrast at 0, 0.5 and 1 h after accumulation of 2PG-S*VVVT-PEG4-ol coated USPIOs at dose of 2.0 mg Fe per kg. **(E, F)** Histopathological analysis of liver of mice after 1 h post intravenous injection of 2PG-S*VVVT-PEG4-ol coated USPIOs at dose of 2.0 mg Fe per kg. Scale bar is 100 μ m.

CONCLUSION

The development of highly biocompatible and performing USPIOs contrast agents dedicated to *in vivo* MRI applications relies strongly on the quality of their coating. We designed a library of short peptides and ligands that are capable of forming highly stable SAMs on the surface of USPIOs. The bisphosphorylated peptides and ligands outperformed their homologues with other known anchor groups

commonly used to cap iron oxide nanoparticles, *e.g.*, DOPA, carboxylic acid. The peptide coated USPIOs were readily prepared with high yields after purification by size-exclusion chromatography (94%) and possessed a narrow hydrodynamic size dispersion (18 ± 8 nm) with near neutral charge (-14 ± 2 mV). With our funnel selection process, we found that 2PG-S*VVVT-PEG4-ol coated USPIOs provided long term stability against electrolyte-induced aggregation in physiological conditions, absence of detectable non-specific binding to live cells and no cytotoxicity at high concentrations. Interestingly, the peptide coated USPIOs demonstrated strong r_1 and r_2 relaxivities and high r_2/r_1 ratios that outperformed commercially available contrast agents. Finally, 2PG-S*VVVT-PEG4-ol coated USPIOs provided strong and lasting contrast enhancement during *in vivo* liver and tumor liver T2-weighted MRI. The development of well-designed peptide coated USPIOs by functionalization with biomarkers will enable, for example, the tracking of specific tissues such as breast cancer tumors and provide targeted contrast agents for early cancer diagnosis by *in vivo* high-resolution contrast-enhanced MRI.

MATERIALS AND METHODS

Materials and Reagents. Oleic acid coated iron oxide nanoparticles in chloroform were purchased from Ocean NanoTech, LLC (San Diego). The alkyl phosphorothioic acid ligands were purchased from Prochimia (ProChimia Surfaces Sp. z o.o., Sopot, Poland). Customized ligands and peptides were purchased from Peptide and Protein Research (PPR Ltd, Hampshire, UK). Dimethyl sulfoxide (99%), ferrozine [3-(2-pyridyl)-5,6-diphenyl-1,2,4-triazine-*p,p'*-disulfonic acid monosodium salt hydrate] (97%), hydroxylamine.HCl, ammonium hydroxide, tetramethylammonium hydroxide (96%) (TMAOH), iron (III) chloride hexahydrate, Tween 20, HEPES and PBS buffers were purchased from Sigma Aldrich (Singapore). FBS and DMEM were purchased from Thermofisher, Life Technologies Holdings PTE LTD (Singapore). Magnevist® was purchased from Zuellig Pharma (Singapore). Nanosep centrifugal devices 10 kDa were purchased from PALL Corp. (Portsmouth, Hants, UK). UV-visible spectra were obtained using a SpectraMax Plus spectrophotometer (Molecular Devices, Oregon, USA) and 384 wells plates from Corning (Lowell, US). Crystal structures of the USPIOs were obtained with a General Area Detector Diffraction System (GADDS) XRD instrument from Bruker. All experiments were conducted using

milliQ water. μ -Slide angiogenesis were obtained from Ibidi. Prussian blue staining was done with 1:1 (v:v) mixture of 5% (w:v) potassium ferrocyanide $K_4Fe(CN)_6 \cdot 3H_2O$ (Sigma) and 2% (v:v) HCl (Merck). Optical imaging was done using a Nikon TS100 microscope system. Cell viability was measured with a Promega CellTiter 96® Aqueous One Solution Cell Proliferation kit. Absorbance at 490 nm was read using the Perkin Elmer EnSpire® Multimode Plate Reader system.

Preparation of tetramethylammonium hydroxide coated USPIOs. In a 15 mL tube, 996 μ L of oleic acid coated USPIOs (10 nm in diameter, 25 mg/mL of Fe) in chloroform were mixed for 30 min at room temperature with 3 mL of 2 mM of TMAOH in water. Chloroform (2 mL) was added and the two phases were separated overnight at 5°C. The aqueous phase containing the TMAOH coated USPIOs was then collected and placed into a 15 mL tube and washed 3 times with 18 mL acetone for 5 min. The TMAOH coated USPIOs were collected by centrifugation (x1000 rpm for 5 min) and dried under a fume hood to remove the remaining solvent. The TMAOH coated USPIOs were then suspended in 4 mL of 0.1 % (w/v) TMAOH in water and stored at 5°C. A Fe content of 93 mM in the TMAOH coated USPIOs stock solution was determined by ferrozine assay.

Preparation of peptide coated USPIOs. To prepare peptide coated USPIOs, 1 volume of 2 mM solution of peptide/ligand (either unitary or mixed) prepared in 25:75 (v/v) DMSO:water was mixed with 0.05 volume of 1% (v/v) Tween 20 in water. Then, 0.1 volume of TMAOH coated USPIOs (93 mM Fe content) in 0.1% (w/v) of TMAOH in water and 8.9 volumes of water were added and mixed at room temperature for an hour. A volume of HEPES 10X buffer (200 mM HEPES, 1 M NaCl, pH 7.4) was added and the solution was mixed at room temperature overnight.

Size-exclusion chromatography. Sephadex G25 superfine (10 mL) was prepared, loaded into a column and stored in 25:75 (v/v) ethanol:water solution. The column was equilibrated with 0.0005% (v/v) Tween 20 in water. A mL peptide coated USPIOs was concentrated to approximately 100 μ L by centrifugation on a 10 kDa cut-off Nanosep filter. Then, the USPIOs were loaded on the column and eluted under gravity using water with 0.0005% (v/v) Tween 20 as the mobile phase. Approximately 1.4 mL colored fractions were collected in the excluded volume.

Calculation of the yield of peptide coated USPIONs. The yield of preparations of peptide coated USPIONs is calculated based on the absorbance at 300 nm of the samples before and after coating and purification by size-exclusion chromatography with G25 resin columns.

$$\text{Yield in \%} = 100 * (A_{300 \text{ after G25}} / A_{300 \text{ control}})$$

$A_{300 \text{ after G25}}$ is the absorbance at 300 nm of the sample after purification with G25 resin and the total volume of the sample adjusted to 1 mL with water. $A_{300 \text{ control}}$ is the absorbance at 300 nm of the same sample before ligand exchange with peptides and the total volume of the sample adjusted to 1 mL with water.

All experiments were repeated at least two times and presented as average and standard deviation.

Normalized aggregation parameter. To allow the comparison of results from different electrolyte-induced aggregation experiments, we defined an aggregation parameter (AP) as follows:

$$\text{AP} = (A_{450\text{nm}} - A_{\text{ref}450\text{nm}}) / (A_{310\text{nm}} - A_{\text{ref}310\text{nm}})$$

$A_{450\text{nm}}$ and $A_{310\text{nm}}$ are absorbance values of solutions of nanoparticles at 450 nm and 310 nm, respectively. The empiric wavelength of 450 nm has been chosen to reflect the aggregated state of the nanoparticles. $A_{\text{ref}450\text{nm}}$ and $A_{\text{ref}310\text{nm}}$ are absorbance values of water at 450 nm and 310 nm. To allow direct comparison of results obtained with different peptide coated USPIONs, this primary aggregation parameter was then normalized by dividing the aggregation parameter values of each experiment by the initial aggregation parameter value of the sample before the stability test. This provided a Normalized Aggregation Parameter (NAP). A stable sample should have a stable UV-visible absorbance spectrum and hence, its NAP is near 1. An increase of the NAP indicated instability and eventually aggregation of the USPIONs.

All experiments were repeated at least two times and presented as average and standard deviation.

Ferrozine assay. A stock solution of 10 mM ferrozine solution was prepared by dissolving 51.4 mg ferrozine (492.46 g/mol) and 1 g hydroxylamine.HCl (69.49 g/mol) in a mixture of 5 mL of HCl (37%, v:v) and 5 mL of water. Ammonium buffer (8 mL, pH 5.5) was prepared by dissolving 20 g ammonium acetate (77.08 g/mol) in 17.50 mL ammonium hydroxide in 50 mL of water before addition of 30 mL HCl (37%, v:v). An iron standard solution at 1 mol/L of Fe was prepared by dissolving 0.067 g $\text{FeCl}_2 \cdot 6\text{H}_2\text{O}$

(270.30 g/mol) in 250 μL of water. Subsequent dilutions of this standard solution were made to prepare a calibration curve.

The iron content in each standard solution and USPIOs preparation was determined by mixing 1 μL of the sample with 100 μL of a 10 mM ferrozine solution and 50 μL water. The samples were heated to 60°C for 30 min. The ammonium buffer solution (350 μL) was added to the sample which was then analyzed by UV-visible spectrometry to prepare a calibration curve and quantify the iron content of each USPIOs sample.

Dynamic light scattering and zeta potential characterization. Dynamic light scattering (DLS) was performed using a Malvern ZetasizerNano ZS instrument equipped with a 633 nm HeNe laser to measure the hydrodynamic particle size and distribution in solution. The characterization of the zeta potential of peptide coated USPIOs was performed with the same instrument through application of a voltage stimulus ranging from -100 to 100 mV between the electrodes of the dual purpose cuvette. A statistical average of three readings per sample was taken for each measurement.

High-resolution transmission electron microscopy. The USPIOs samples were diluted into ethanol (for the oleic acid coated USPIOs in chloroform) or water (for the TMAOH and peptide coated USPIOs) and deposited on Ultrathin Carbon (<3 nm) on Carbon Holey support film TEM grids (Ultrathin Carbon / Holey Support on 400 mesh, Pelco International, USA). The USPIOs were analysed with a Philips CM300 high resolution analytical TEM/STEM. The core size of the USPIOs was determined with ImageJ v1.47e software using the macro 'ParticleSizeAnalyzer'. A minimum of 100 USPIOs were counted to determine the size distribution of the sample.

Cell viability assay. PLC/PRF5 cells were dissociated using trypsin and counted. The cells were then washed and suspended at a density of 400,000 cells per mL in Dulbecco's minimal Eagle's medium (DMEM) with 5 % (v/v) fetal bovine serum (FBS) (v:v). Aliquots (50 μL , 20,000 cells) were placed in each well of 96 well flat bottom plates. The cells were allowed to adhere overnight at 37°C.

The USPIOs dispersed in 0.0005% (v/v) Tween 20 in water were diluted in Dulbecco's minimal Eagle's medium (DMEM) with 10 % (v/v) fetal bovine serum (FBS) to prepare a series of samples

containing between 400 ng/mL and 200 $\mu\text{g/mL}$ of Fe. Each USPIOs solution (50 μL) was added to the cells in the 96 well plates and incubated for 48 hours at 37°C.

Cell growth was used as a proxy for cytotoxicity and was measured using a CellTiter 96® AQueous One Solution Cell Proliferation Assay (MTS). The growth of treated cells growth was reported as a percentage of the control untreated cells. All experiments were repeated at least three times and presented as average and standard deviation.

Cell non-specific binding. PLC/PRF5 cells were dissociated using trypsin and counted. The cells were then washed and suspended at a density of 10^6 cells per mL. Aliquots (50 μL , 20,000 cells) were seeded in each well in a μ -Slide plate from Ibidi. The cells were allowed to adhere overnight at 37°C.

Peptide coated USPIOs in 0.0005% (v/v) Tween 20 in water were diluted in Dulbecco's minimal Eagle's medium (DMEM) with 10 % (v/v) fetal bovine serum (FBS) (v:v) to prepare samples containing 10 $\mu\text{g/mL}$ to 100 $\mu\text{g/mL}$ of Fe. The medium from each well was removed and replaced with 50 μL of USPIOs solution and incubated overnight at 37°C.

The medium containing the USPIOs was washed away from the wells thoroughly with PBS. The cells were then fixed with a 4% (v/v) paraformaldehyde solution in PBS for 15 min at room temperature. The excess paraformaldehyde was removed by washing with water. Prussian blue staining reagent (50 μL) containing 2.5% (w/v) potassium ferrocyanide trihydrate ($\text{K}_3\text{Fe}(\text{CN})_6 \cdot 3\text{H}_2\text{O}$) in water and 1% (v/v) HCl were added to each well and incubated at room temperature for 30 min. The staining reagent was then thoroughly washed away with water. The cells were counterstained for 30 min at room temperature with 50 μL of Nuclear Fast Red solution in water. The excess of solution was then removed by washing away with water. The non-specific association of the USPIOs to the cells was finally visualized by light microscope.

Magnetic resonance imaging phantom. Peptide coated USPIOs and the commercial MRI contrast agents Magnevist® and Resovist® were serially diluted in 500 μL of water to give 5 concentrations of

iron or gadolinium in the case of Magnevist®. The phantoms were then prepared in 1 mL syringes by filling them to 0.4 mL mark and sealing the ends with parafilm.

The magnetic resonance relaxivities r_1 and r_2 of peptide coated USPIOs and the commercial MRI contrast agents Magnevist® and Resovist® were determined using a 7 Tesla Bruker ClinScan magnetic resonance imaging system. T1 relaxation times were determined by an inversion recovery experiment with a number of inversion times (TI) (9 TIs; TI: 41–4000 ms; repetition time (TR): 5000 ms; echo time (TE): 7.7 ms). T2 relaxation times were determined from a multiecho spin-echo sequence (TR: 4000 ms; TE: 17.9-250.6 ms). The longitudinal (r_1) and transverse (r_2) relaxivities were obtained from the slope of $1/T1$ or $1/T2$ *versus* molar concentration plots.

Contrast enhancement in muscle. All animal experiments were approved by the Institutional Animal Care and Use Committee (IACUC #151089). *In vivo* MRI was performed using NCr nude mouse as a model. Peptide coated USPIOs were diluted in saline to a concentration of 0.2 mg Fe per mL. The USPIOs were injected intramuscularly into the left hind limb of the animal at a dose of 1 mg Fe per kg of mouse body weight. The transverse and coronal plane images were scanned using a 7T Bruker Clinscan with the following parameters: T2-weighted turbo spin echo sequence TSE, TR/TE=1010/56 ms, 320x320 matrices, slice thickness = 0.8 mm, averages = 2.

Liver magnetic resonance imaging. *In vivo* MRI of liver were performed using NCr nude mouse as a model. Peptide coated USPIOs were diluted in saline to a concentration of 0.2 mg Fe per mL. The USPIOs were injected intravenously in the tail vein at a dose of 1 mg Fe per kg of mouse body weight. The transverse and coronal plane images were scanned at pre-injection, 30 mins and 60 mins post-injection using a 7T Bruker Clinscan (n=3) with the following parameters: T2 weighted turbo spin echo sequence TSE, TR/TE=1010/56 ms, 320 x 320 matrices, slice thickness = 1 mm, averages = 2 (transverse), 4 (coronal).

The SNR (signal-to-noise ratio) was calculated using the equation:

$$SNR_{liver} = SI_{liver} / SD_{noise}$$

where SI represents signal intensity and SD represents s.d. The SNR changes of the ROI was calculated by the equation:

$$\Delta\text{SNR}=(\text{SNR}_{\text{post}}-\text{SNR}_{\text{pre}})/\text{SNR}_{\text{pre}}.$$

The experiment was repeated three times and presented as average and standard deviation.

Detection of liver tumor by magnetic resonance imaging. The orthotopic liver tumor model was established by inoculation of PLC/PRF5 cells into the liver of nude mice. When the tumors reached 5 mm in diameter, *in vivo* MRI of liver was performed. The USPIOs were injected intravenously in the tail vein at a dose of 2 mg Fe per kg of mouse body weight. The axial, coronal and sagittal planes were scanned at 0, 30 and 60 min post injection using a 9.4T Bruker Biospec (n=3). T2-weighted, turboRARE sequence, TR/TE= 570/23ms, 320 x 320 matrices, slice thickness = 1 mm, averages = 2, Rare factor = 8.

The SNR was calculated using the equation:

$$\text{SNR}_{\text{liver}}=\text{SI}_{\text{liver}}/\text{SD}_{\text{noise}}$$

where SI represents signal intensity and SD represents s.d.

CNR (contrast-to-noise ratio) was calculated using the formula:

$$\text{CNR} = (\text{SNR}_{\text{tumour}} - \text{SNR}_{\text{liver}}) / \text{SNR}_{\text{tumour}}.$$

The experiment was repeated three times and presented as average and standard deviation.

ASSOCIATED CONTENT

Supporting Information. Stability evaluation against electrolyte-induced aggregation of single and mixed peptide coated USPIOs, magnetic resonance phantom measurements and intramuscular magnetic resonance imaging. This material is available free of charge *via* the Internet at <http://pubs.acs.org>.

Conflict of Interest. The authors declare no competing financial interest.

AUTHOR INFORMATION

Corresponding author

*paramelled@imre.a-star.edu.sg

ORCID

David Paramelle: 0000-0002-5388-9339

Author contributions

D.P. conceived and supervised the investigation, designed the peptide library and the protocols for the preparation and evaluation of the peptide coated USPIOs, analyzed the data and wrote the manuscript. H.L.C. and C.R.R.G. contributed to the design of the protocols for the preparation of peptide coated USPIOs, prepared and tested the peptide coated USPIOs. M.N. performed the MRI experiments. L.L. performed the *in vitro* evaluation. D.G.F. contributed to the design of the peptide library. K.B. contributed to the design and supervision of the MRI evaluation. All authors made corrections and provided critical feedback on the manuscript. All authors have given approval to the final version of the manuscript. ‡These authors contributed equally.

ACKNOWLEDGMENT

The authors would like to acknowledge the Joint Council Career Development Award funding from the Agency for Science, Technology and Research (A*STAR) – Grant Number 14302FG094 and DGF support from North West Cancer Research. All animal experiments were approved by the Institutional Animal Care and Use Committee (IACUC #151089).

REFERENCES

1. Smith, B. R.; Gambhir, S. S. Nanomaterials for *In Vivo* Imaging. *Chem. Rev.* **2017**, *117*, 901–986.
2. Datta, N. R.; Krishnan, S.; Speiser, D. E.; Neufeld, E.; Kuster, N.; Bodis, S.; Hofmann, H. Magnetic Nanoparticle-Induced Hyperthermia with Appropriate Payloads: Paul Ehrlich’s “Magic (Nano)Bullet” for Cancer Theranostics? *Cancer Treat. Rev.* **2016**, *50*, 217–227.
3. Arami, H.; Khandhar, A.; Liggitt, D.; Krishnan, K. M. *In Vivo* Delivery, Pharmacokinetics, Biodistribution and Toxicity of Iron Oxide Nanoparticles. *Chem. Soc. Rev.* **2015**, *44*, 8576–8607.
4. Lee, N.; Yoo, D.; Ling, D.; Cho, M. H.; Hyeon, T.; Cheon, J. Iron Oxide Based Nanoparticles for Multimodal Imaging and Magnetoresponse Therapy. *Chem. Rev.* **2015**, *115*, 10637–10689.

5. Jin, R.; Lin, B.; Li, D.; Ai, H. Superparamagnetic Iron Oxide Nanoparticles for MR Imaging and Therapy: Design Considerations and Clinical Applications. *Curr. Opin. Pharmacol.* **2014**, *18*, 18–27.
6. Gallo, J.; Long, N. J.; Aboagye, E. O. Magnetic Nanoparticles as Contrast Agents in the Diagnosis and Treatment of Cancer. *Chem. Soc. Rev.* **2013**, *42*, 7816.
7. Hilger, I.; Kaiser, W. A. Iron Oxide-Based Nanostructures for MRI and Magnetic Hyperthermia. *Nanomedicine* **2012**, *7*, 1443–1459.
8. Rosen, J. E.; Chan, L.; Shieh, D.-B.; Gu, F. X. Iron Oxide Nanoparticles for Targeted Cancer Imaging and Diagnostics. *Nanomedicine Nanotechnology, Biol. Med.* **2012**, *8*, 275–290.
9. Qiao, R.; Yang, C.; Gao, M. Superparamagnetic Iron Oxide Nanoparticles: From Preparations to *in Vivo* MRI Applications. *J. Mater. Chem.* **2009**, *19*, 6274.
10. Laurent, S.; Forge, D.; Port, M.; Roch, A.; Robic, C.; Vander Elst, L.; Muller, R. N. Magnetic Iron Oxide Nanoparticles: Synthesis, Stabilization, Vectorization, Physicochemical Characterizations, and Biological Applications. *Chem. Rev.* **2008**, *108*, 2064–2110.
11. Neuwelt, E. a; Hamilton, B. E.; Varallyay, C. G.; Rooney, W. R.; Edelman, R. D.; Jacobs, P. M.; Watnick, S. G. Ultrasmall Superparamagnetic Iron Oxides (USPIOs): A Future Alternative Magnetic Resonance (MR) Contrast Agent for Patients at Risk for Nephrogenic Systemic Fibrosis (NSF)? *Kidney Int.* **2009**, *75*, 465–474.
12. Bobo, D.; Robinson, K. J.; Islam, J.; Thurecht, K. J.; Corrie, S. R. Nanoparticle-Based Medicines: A Review of FDA-Approved Materials and Clinical Trials to Date. *Pharm. Res.* **2016**, *33*, 2373–2387.
13. Tong, S.; Hou, S.; Zheng, Z.; Zhou, J.; Bao, G. Coating Optimization of Superparamagnetic Iron Oxide Nanoparticles for High T₂ Relaxivity. *Nano Lett.* **2010**, *10*, 4607–4613.

14. Gupta, A. K.; Gupta, M. Synthesis and Surface Engineering of Iron Oxide Nanoparticles for Biomedical Applications. *Biomaterials* **2005**, *26*, 3995–4021.
15. Palui, G.; Aldeek, F.; Wang, W.; Mattoussi, H. Strategies for Interfacing Inorganic Nanocrystals with Biological Systems Based on Polymer-Coating. *Chem. Soc. Rev.* **2015**, *44*, 193–227.
16. Boyer, C.; Whittaker, M. R.; Bulmus, V.; Liu, J.; Davis, T. P. The Design and Utility of Polymer-Stabilized Iron-Oxide Nanoparticles for Nanomedicine Applications. *NPG Asia Mater.* **2010**, *2*, 23–30.
17. Free, P.; Paramelle, D.; Bosman, M.; Hobley, J.; Fernig, D. G. Synthesis of Silver Nanoparticles with Monovalently Functionalized Self-Assembled Monolayers. *Aust. J. Chem.* **2012**, *65*, 275.
18. Chen, X.; Qoutah, W. W.; Free, P.; Hobley, J.; Fernig, D. G.; Paramelle, D. Features of Thiolated Ligands Promoting Resistance to Ligand Exchange in Self-Assembled Monolayers on Gold Nanoparticles. *Aust. J. Chem.* **2012**, *65*, 266.
19. Paramelle, D.; Sadovoy, A.; Gorelik, S.; Free, P.; Hobley, J.; Fernig, D. G. A Rapid Method to Estimate the Concentration of Citrate Capped Silver Nanoparticles from UV-Visible Light Spectra. *Analyst* **2014**, *139*, 4855.
20. Duchesne, L.; Gentili, D.; Comes-Franchini, M.; Fernig, D. G. Robust Ligand Shells for Biological Applications of Gold Nanoparticles. *Langmuir* **2008**, *24*, 13572–13580.
21. Lévy, R.; Thanh, N. T. K.; Doty, R. C.; Hussain, I.; Nichols, R. J.; Schiffrin, D. J.; Brust, M.; Fernig, D. G. Rational and Combinatorial Design of Peptide Capping Ligands for Gold Nanoparticles. *J. Am. Chem. Soc.* **2004**, *126*, 10076–10084.
22. Paramelle, D.; Nieves, D.; Brun, B.; Kraut, R. S.; Fernig, D. G. Targeting Cell Membrane Lipid Rafts by Stoichiometric Functionalization of Gold Nanoparticles with a Sphingolipid-Binding Domain Peptide. *Adv. Healthc. Mater.* **2015**, *4*, 911–917.

23. Paramelle, D.; Peng, T.; Free, P.; Fernig, D. G.; Lim, S.; Tomczak, N. Specific Internalisation of Gold Nanoparticles into Engineered Porous Protein Cages *via* Affinity Binding. *PLoS One* **2016**, *11*, e0162848.
24. Amstad, E.; Gillich, T.; Bilecka, I.; Textor, M.; Reimhult, E. Ultrastable Iron Oxide Nanoparticle Colloidal Suspensions Using Dispersants with Catechol-Derived Anchor Groups. *Nano Lett.* **2009**, *9*, 4042–4048.
25. Queffélec, C.; Petit, M.; Janvier, P.; Knight, D. A.; Bujoli, B. Surface Modification Using Phosphonic Acids and Esters. *Chem. Rev.* **2012**, *112*, 3777–3807.
26. Lartigue, L.; Innocenti, C.; Kalaivani, T.; Awwad, A.; Sanchez Duque, M. D. M.; Guari, Y.; Larionova, J.; Guérin, C.; Montero, J.-L. G.; Barragan-Montero, V.; Arosio, P.; Lascialfari, A.; Gatteschi, D.; Sangregorio, C. Water-Dispersible Sugar-Coated Iron Oxide Nanoparticles. An Evaluation of Their Relaxometric and Magnetic Hyperthermia Properties. *J. Am. Chem. Soc.* **2011**, *133*, 10459–10472.
27. Krenkova, J.; Foret, F. Iron Oxide Nanoparticle Coating of Organic Polymer-Based Monolithic Columns for Phosphopeptide Enrichment. *J. Sep. Sci.* **2011**, *34*, 2106–2112.
28. Wu, M.; Guo, Q.; Xu, F.; Liu, S.; Lu, X.; Wang, J.; Gao, H.; Luo, P. Engineering Phosphopeptide-Decorated Magnetic Nanoparticles as Efficient Photothermal Agents for Solid Tumor Therapy. *J. Colloid Interface Sci.* **2016**, *476*, 158–166.
29. Barch, M.; Okada, S.; Bartelle, B. B.; Jasanoff, A. Screen-Based Analysis of Magnetic Nanoparticle Libraries Formed Using Peptidic Iron Oxide Ligands. *J. Am. Chem. Soc.* **2014**, *136*, 12516–12519.
30. Busquets, M. A.; Estelrich, J.; Sánchez-Martín, M. J. Nanoparticles in Magnetic Resonance Imaging: From Simple to Dual Contrast Agents. *Int. J. Nanomedicine* **2015**, *10*, 1727.

31. Reimer, P.; Balzer, T. Ferucarbotran (Resovist): A New Clinically Approved RES-Specific Contrast Agent for Contrast-Enhanced MRI of the Liver: Properties, Clinical Development, and Applications. *Eur. Radiol.* **2003**, *13*, 1266–1276.
32. Zhao, Z.; Zhou, Z.; Bao, J.; Wang, Z.; Hu, J.; Chi, X.; Ni, K.; Wang, R.; Chen, X.; Chen, Z.; Gao, J. Octapod Iron Oxide Nanoparticles as High-Performance T2 Contrast Agents for Magnetic Resonance Imaging. *Nat. Commun.* **2013**, *4*, 2266.

Table of Contents Graphic

